Int. J. Electrochem. Sci., 14 **(2019)** 5211 – 5225, doi: 10.20964/2019.06.62

International Journal of
ELECTROCHEMICAL
SCIENCE
www.electrochemsci.org

Degradation of Titanium Electrodes in the Alternating Polarity Electrolysis

Pavel S. Shlepakov[1], *Ilia V. Uvarov*[1,*], *Victor V. Naumov*[1], *Leonid A. Mazaletskiy*[1,2], *Vitaly B. Svetovoy*[3,4]

[1] Laboratory of Micro- and Nanosystem Technology, Valiev Institute of Physics and Technology of Russian Academy of Sciences, Yaroslavl Branch, Universitetskaya 21, 150007 Yaroslavl, Russia
[2] P.G. Demidov Yaroslavl State University, Sovetskaya 14, 150003 Yaroslavl, Russia
[3] Zernike Institute for Advanced Materials, University of Groningen – Nijenborgh 4, 9747 AG Groningen, The Netherlands
[4] A.N. Frumkin Institute of Physical Chemistry and Electrochemistry RAS, Leninsky pr. 31, 199071 Moscow, Russia
[*]E-mail: i.v.uvarov@bk.ru

Received: 7 March 2019 / *Accepted:* 9 April 2019 / *Published:* 10 May 2019

Electrolysis of water performed by microsecond voltage pulses of alternating polarity has been used to generate nanobubbles in microscopic systems. These nanobubbles exhibit interesting and useful effects, but their production requires a high current density of >10 A/cm^2. Deposited platinum or gold electrodes cannot withstand these conditions for a long time. Titanium showed the best durability, although it also undergoes degradation. The mechanism of degradation differs from that in usual DC electrolysis and was not previously explored. In this paper, the wear of thin film titanium electrodes fabricated on a silicon substrate by surface micromachining is investigated. The electrodes are tested in the alternating polarity process of various frequencies and durations. They are oxidized during operation, but the spatial distribution and chemical composition of the oxide differ from those observed in normal electrolysis. The strongest oxidation occurs at the edges of the electrodes, while the central part is less involved. At a high frequency of voltage pulses (400 kHz) the electrodes are oxidized much less than at low frequency (50–100 kHz). The oxide grows due to misbalance between periodic oxidation and reduction processes. Internal mechanical stress generated due to oxidation causes degradation of the electrodes.

Keywords: Water electrolysis; Alternating polarity; Electrodes; Oxidation; Degradation;

1. INTRODUCTION

Electrochemical decomposition of water has been known for more than 200 years [1, 2] and has many applications including the production of hydrogen [3, 4] and oxygen [5, 6] for various

purposes. Recently, a special regime of water electrolysis performed by microsecond voltage pulses of alternating polarity (AP) was demonstrated [7]. Unlike usual DC electrolysis, where hydrogen is produced at the cathode and oxygen is generated at the anode, in the AP process both H_2 and O_2 gases are produced above each electrode. Switching the voltage polarity at a frequency of ~100 kHz limits the size of the gas bubbles by the value of about 100 nm [8]. These bubbles are invisible optically due to their small size, but their collective effects are well observable. A significant reduction of the refractive index of liquid enriched with nanobubbles was demonstrated [9]. Furthermore, a cloud of nanobubbles floating in the electrolyte volume was generated and visualized [8]. Densely packed H_2 and O_2 nanobubbles can merge into a microbubble that explodes with the release of a large amount of energy [10]. Short-time AP electrolysis can be used as a working principle for a fast electrochemical actuator [11]. When the nanobubbles are generated in a microchamber covered by a flexible membrane, the pressure in the chamber increases and pushes the membrane up. When the voltage pulses are switched off, the produced gas is terminated very quickly due to the spontaneous combustion of hydrogen and oxygen in nanobubbles [7]. The pressure in the chamber is released in about 1 ms, while in conventional actuators based on the DC electrolysis the gas termination takes minutes [12-19].

An important feature of the short-time AP electrolysis is the homogeneous nucleation of the nanobubbles that occurs due to extremely high supersaturation (~1000) in the vicinity of the electrodes [20]. This supersaturation is provided by the fast change of the voltage polarity and the high current density (~100 A/cm^2). Such a high current density can be achieved easily in microscopic systems, where the electrodes have the size of several tens of micrometers [7-9, 11]. However, long-term production of the nanobubbles is limited by the degradation of the electrodes. Most metals cannot withstand the current density in the AP process. This issue is especially important for practical applications such as electrochemical actuators and pumps since the stability of the electrodes determines the reliability of the device.

Actuators based on the DC process typically utilize electrodes fabricated from chemically inert and corrosion resistant metals, such as platinum [12-16] or gold [17-19]. However, the current density achieved in such devices is usually quite low (< 0.1 A/cm^2) [12, 14, 17]. The AP process destroys platinum electrodes in a few minutes [21], while gold structures degrade even faster [20]. Empirically it was found that titanium electrodes demonstrated the best durability. They become black during the operation that is accompanied by a decrease of the Faraday current, but significant destruction is not observed for hours of continuous work [11]. In this paper, wear of titanium electrodes is investigated in detail. We change the frequency of the driving pulses and duration of the electrochemical process and identify the main degradation mechanisms. This information is useful for choosing optimal operation conditions, which reduce the rate of degradation and increase the lifetime of the electrodes.

2. EXPERIMENTAL

The design of the electrodes is an important factor that determines their efficiency and durability [22]. Circular electrodes withstand several hours in the AP process without significant

degradation [11]. However, for research purposes, it is desirable to accelerate the damage and to localize it to a certain place on the electrode. It is known that the most intensive destruction occurs at the areas with the highest current density, i.e. at protrusions and corners. In this work we choose the shape of isosceles triangles with their vertices facing each other (Fig. 1a). The strongest damage is expected at the vertices. Triangles with a base width of 100 and 200 μm are used. In both cases, the distance between the vertices is 50 μm, and the angle at the vertex is 90°. A cross-section of the electrodes indicating the structural materials is shown schematically in Fig. 1b. Titanium electrodes with a thickness of 100 nm are fabricated on oxidized silicon wafers. Such a small thickness is chosen to speed up the destruction. The contact lines connecting the electrodes with the contact pads are covered by a layer of aluminum, which reduces their resistance. Aluminum is isolated from the electrolyte by a layer of photoresist SU-8.

First, a 0.9 μm thick insulating SiO_2 layer is grown by thermal oxidation of the wafer in wet oxygen. Next, Ti layer with a thickness of 100 nm is deposited by magnetron sputtering. An adhesive underlayer is not required since titanium has strong adhesion to SiO_2. The substrate is covered by the photoresist Shipley S1813 and the UV contact photolithography is performed followed by the etching of the Ti layer in a mixture of nitric and hydrofluoric acids through the photoresistive mask. Then, a 500 nm thick Al layer is deposited. Photolithography and wet etching are performed in order to form the highly conductive layer above the connecting lines and the contact pads. At the last stage, the contact lines (but not contact pads) are covered by 8 μm thick layer of the negative photoresist SU-8 3005.

After fabrication the wafer is divided into samples with a size of 8×20 mm^2. A sample is fixed in a holder and tungsten needles are placed on the contact pads. A droplet of electrolyte (a molar solution of sodium sulfate Na_2SO_4 in distilled water) with a diameter of 5-7 mm is put on the sample covering the electrodes. The sample ready for the test is shown in Fig. 2. The electrochemical process is performed by square voltage pulses of alternating polarity applied to the electrodes. One electrode is grounded while the other one is at positive or negative potential with respect to the ground. Duration of the process varies from 5 to 160 s depending on the experiment. The frequency of the pulses is in the range from 50 to 400 kHz. The pulses have fixed amplitude of 9 V. This amplitude provides significant wear during the selected time interval. At the same time, it is not large enough to cause explosions of microbubbles [11], which can strongly damage the sample. The voltage is provided by a waveform generator Tektronix AFG1022 and amplified 10 times using a homemade power amplifier [23]. The voltage and current flowing through the electrolyte are recorded by a Pico-Scope 5000.

After the electrochemical process the sample is rinsed in distilled water and dried with nitrogen. The degradation is estimated visually using an optical microscope and a camera Moticam 1SP mounted on the eyepiece. Details of the surface and chemical composition of the electrodes are investigated using SEM Zeiss Supra 40 and energy-dispersive X-ray (EDX) spectrometer Oxford Instruments INCA X-act. Normally, observation of the surface is carried out at an accelerating voltage of 20 kV. In order to measure the chemical composition of thin titanium film it is reduced to 4 kV. At this value the penetration depth of electrons into the sample is smaller and the X-ray signal is collected mainly from the film.

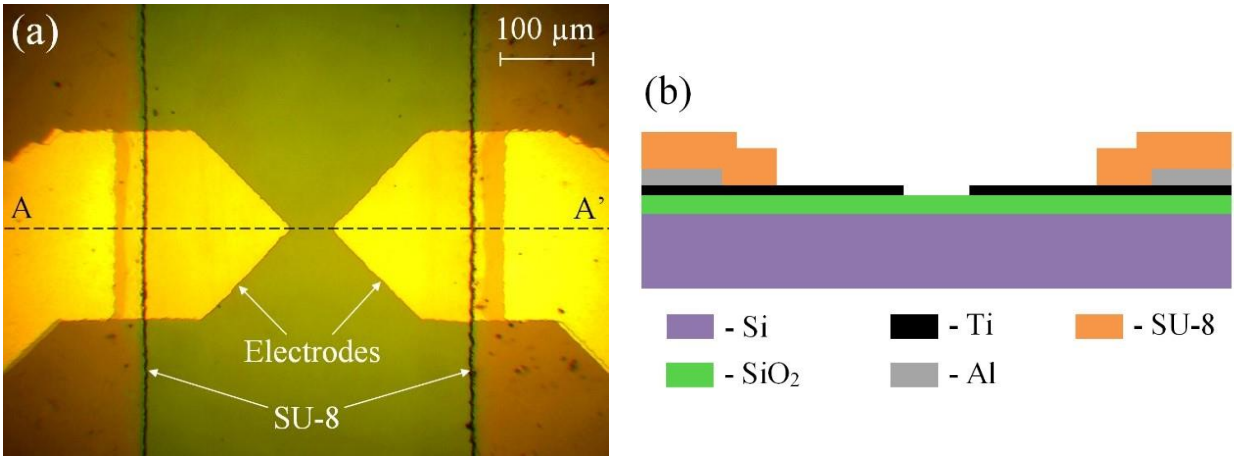

Figure 1. Design of the electrodes: (a) optical image, top view; (b) schematic cross-section along the line AA' shows the structure of the layers.

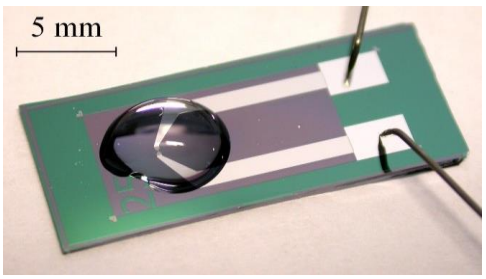

Figure 2. Photo of a sample with the needles touching the contact pads and a droplet of electrolyte covering the electrodes.

3. RESULTS AND DISCUSSION

3.1 Degradation at various frequencies and durations

The dependence of the degradation on the frequency of the driving pulses f is investigated using 100 µm wide electrodes. The electrolysis is performed at f = 50, 100, 200 and 400 kHz. In all cases, the process duration was 60 s. Optical images of the electrodes tested at different f are shown in Fig. 3. The degradation manifests itself as a darkening of the electrode. This phenomenon is observed at all frequencies, but at higher f it is less pronounced. The edges darken stronger than the central part. The width of the darkened area at the edge decreases with increasing f. Partial removal of the electrodes from the substrate is observed at the frequencies of 50 and 100 kHz. As expected, the strongest damage occurs at the vertices of the triangles due to the highest current density.

The time dependence of the degradation is studied on the 200 µm wide electrodes at f = 200 kHz. The duration T of the AP process varies from 5 to 160 s. Optical images of the samples exposed to electrolysis with various T are shown in Fig. 4. An increase in the exposure time makes the electrodes darker. The darkening begins at the edges and then propagates to the central part. The

strongest change of color occurs in the first 40 s of electrolysis. A longer process does not change the appearance of the electrodes significantly.

The electrodes change color due to the formation of some surface layers. It is known [24] that in the DC process an oxide film formed on the titanium anode changes the color due to light interference. At the initial stage of growth the film is yellow, and then turns brown as the thickness increases [24, 25]. In order to verify this effect, we tested a 100 μm wide sample in the DC regime. A positive potential of 9 V was applied to the working electrode during 60 s. The anode obtained a strongly pronounced brown color (see Fig. 5). In the AP process, each electrode periodically plays the role of anode and, therefore, undergoes oxidation. To all appearance formation of the oxide layer causes the darkening of both electrodes. However, the AP mode has a few distinctive features compared to DC electrolysis. First, the edges of the electrode tested in the AP process are usually darker than the central part, while the anode is colored uniformly in the DC mode. Second, at lower frequency of pulses the electrodes change color more intensely than at higher frequency. Third, at lower frequency the electrodes are partially removed from the substrate. These phenomena are not observed in the DC process at the same voltage. To explain these features, it is necessary to consider the surface morphology and chemical composition of the electrodes, and the current flowing through the electrochemical cell.

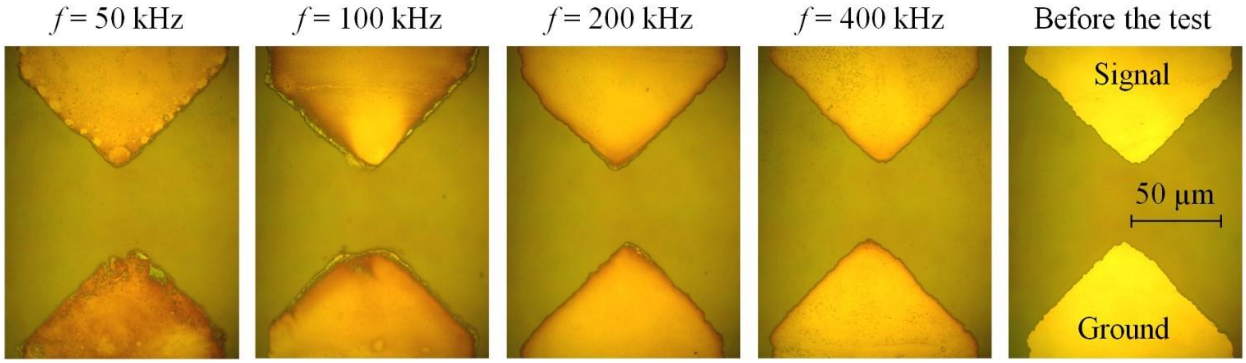

Figure 3. Optical images of the electrodes tested in the AP process at various frequencies during 60 s. The pulses were applied to the upper electrode while the lower electrode was grounded. The image on the right shows the sample before the test.

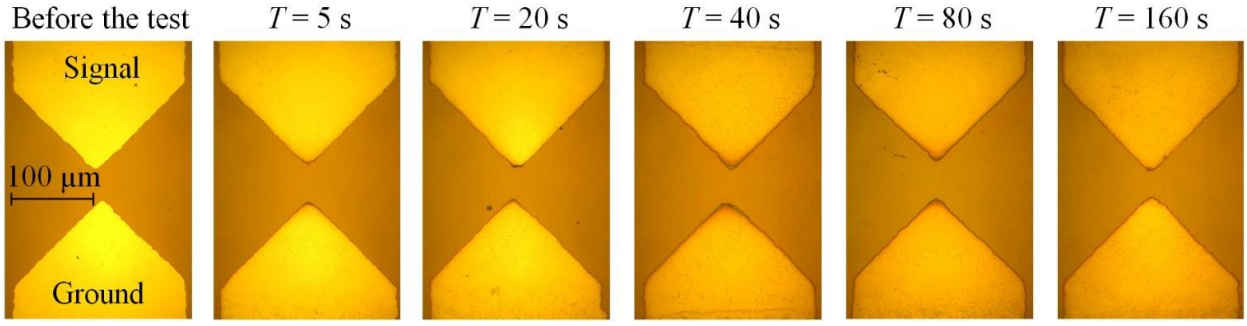

Figure 4. Optical images of the electrodes tested in the AP process of various duration. The frequency of pulses is 200 kHz. The image on the left shows the sample before the test.

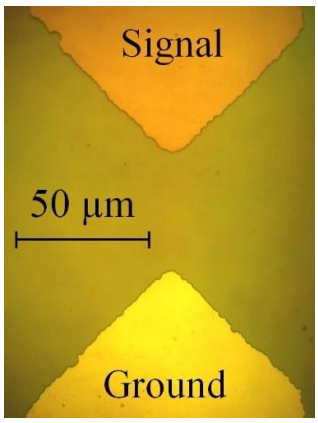

Figure 5. Optical image of the electrodes tested in the DC process. Constant potential of 9 V was applied to the signal electrode during 60 s.

3.2 Investigation of the electrode surface with SEM

SEM images of the electrodes exposed to the AP process are shown in Fig. 6a-d. One can see damaged edges for samples tested at f = 50 and 100 kHz. At f = 200 kHz the damage is smaller but visible at an angle of 20° to the substrate. Practically there is no destruction only at a frequency of 400 kHz. The DC process does not damage the electrodes at all (see Fig. 6e, f).

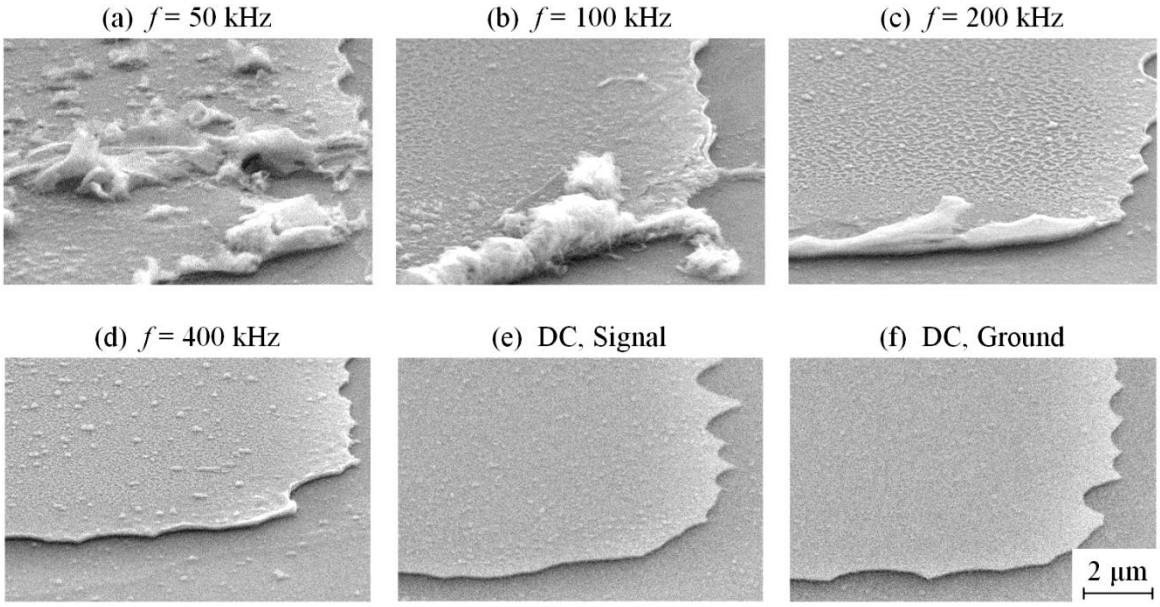

Figure 6. SEM images of the electrodes exposed to the electrolysis during T = 60 s. The images are captured at the angle of 20° with respect to the substrate plane, magnification is 10000x. (a-d) The AP process at different f. Only the grounded electrode is shown. (e, f) The signal and ground electrodes after the DC process.

Three zones of different surface morphology can be distinguished at the electrodes tested in the AP regime. The schematic arrangement of these zones and the corresponding SEM images of the surface are shown in Fig. 7. The central part of the electrode is covered by separate particles with a

lateral size of 50-200 nm (zone I). Closer to the edge the particles become larger and merge with each other, forming a «net» (zone II). In close proximity to the edge the net turns into a continuous layer (zone III). In certain places the layer has small cracks, which allow estimation of its thickness as 50-100 nm. More precise measurement of the thickness by observing cross-section of the electrode in SEM is complicated, because the images of the thin Ti film on the thick SiO_2 layer in the presence of dielectric SU-8 layer have poor resolution due to charging effects. Transition from the net to the continuous layer can be seen in Fig. 6c. These zones are observed at all frequencies except of f = 50 kHz. At this small frequency almost the entire electrode is covered by a continuous layer. With the frequency increase, the zone III narrows. At f = 100 kHz it has a width of about 10 μm, at f = 400 kHz the width is about 4 μm. Comparison of the SEM images with the optical snapshots in Fig. 3 shows that the areas covered by the continuous layer are darker than the central part.

The electrodes exposed to the DC process have homogeneous surface morphology all over the area of the electrode. This corresponds to the uniform color distribution in the optical image (Fig. 5). Grains with a size of 20-30 nm are visible at the cathode. At the anode the grains are undistinguishable and the surface looks very smooth.

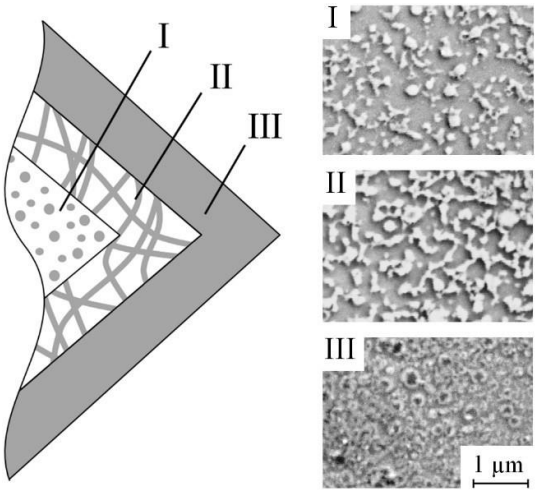

Figure 7. Schematic image of the electrode indicating the zones of different surface morphology: I individual particles are located on the surface; II the surface is covered by a net; III the electrode is covered by a continuous layer. SEM images on the right show typical appearance of the areas. Magnification is 30000x.

3.3 Chemical composition of the electrodes

EDX analysis confirms that the darkening of the signal electrode in the DC process is caused by the oxidation of titanium. The chemical composition of the electrodes shown in Fig. 5 is presented in Table 1. The anode contains much more oxygen than the cathode (22 and 3 at. %, respectively). At the same time, the anode contains less titanium and silicon because the oxide partially protects the unoxidized Ti layer and SiO_2 substrate from the bombarding electrons and attenuates the radiation coming from these layers. A small amount of carbon is present due to contamination and carbon-

containing residues (the photoresist) after the fabrication. The presented data is obtained at the central part of the electrodes, but the same chemical composition is observed over the entire area.

Chemical composition of the electrode tested in the AP process at f = 100 kHz is also shown in Table 1. The percentage of oxygen is increased in both electrodes compared to the unoxidized cathode from the DC process, but unlike the oxidized anode oxygen is distributed non-uniformly. The smallest content is observed in the central region with individual particles (zone I, Fig. 7), and the largest content is found at the edge covered by a continuous layer (zone III). In addition, an increased percentage of carbon and fluorine is observed in the electrode material. A certain amount of F can remain in the sample after the etching of Ti in hydrofluoric acid. Carbon in the sample originates from the photoresist. The amount of O, C, and F increases from the center of electrode to the edge. One can conclude that the material covering the electrode contains all these elements. The more continuous the coverage, the higher the amount of C, O, and F in the chemical composition.

In order to investigate the material covering the electrode in the AP process, the X-ray spectra of a particle located in zone I and the surface of the electrode between the particles have been measured (Fig. 8). One can see that the peaks corresponding to C, O and F in the particle spectrum are higher than in the surface spectrum. The difference in peak height was expected to be more significant. However, the particles are located quite densely (see the inset in Fig. 8). EDX analysis with an accelerating voltage of 4 kV excites atoms located in a radius of about 200 nm around the region of analysis. During the measurement of the free surface spectrum, neighboring particles entered into the excitation region, and their radiation contributed to the height of the C, O, and F peaks. It is important that the Ti peak has the same height in both spectra. This means that titanium is contained not only in the electrode, but also in the particle. Thus, the material formed on the electrodes contains mainly oxygen and titanium and some traces of C and F. Since Ti is easily oxidized we expect that the material covering the electrode is titanium oxide with carbon and fluorine inclusions. The oxide is collected in the individual particles at the central part of the electrode, while at the edge it forms a continuous layer.

Table 1. Chemical composition of the electrodes exposed to the electrolysis during T = 60 s. The content of chemical elements is given in atomic percent. In the case of the DC process, the EDX analysis is performed in the central part of the electrodes. For the AC process, it is carried out in the zones I, II, and III of the grounded electrode. The region of analysis has the size of $3.5 \times 2.5\ \mu m^2$.

Chemical element	DC electrolysis		AP electrolysis (100 kHz)		
	Signal	Ground	Area I	Area II	Area III
C	1.2	1.9	2.6	4.0	6.1
O	21.8	2.9	18.7	24.9	30.2
F	-	-	1.9	3.5	5.0
Si	1.1	1.5	1.4	1.2	0.9
Ti	75.9	93.7	75.2	65.9	57.4

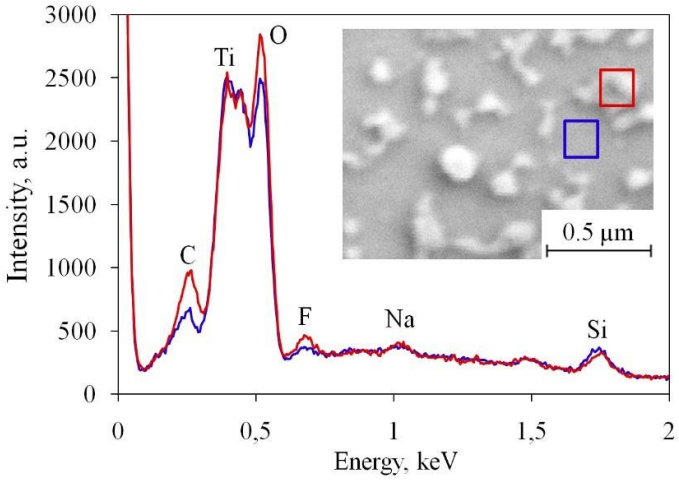

Figure 8. Energy spectra of the electrode tested in the AP process at f = 100 kHz during T = 60 s. The inset shows the SEM image of the surface with the location of the EDX analysis regions. The spectrum is measured on the particle (red color) and on a free surface (blue color). The region of analysis has a size of 150×150 nm^2.

Non-uniform distribution of the oxide can be explained as follows. Titanium is oxidized during one half of the period of the driving pulse. The current density is higher at the edge of the electrode than in the central part. Therefore, more oxygen is generated, and a larger volume of titanium oxide grows at the edge. During the second half, titanium is reduced from the oxide. However, it is harder to reduce Ti that lies deep in the oxide layer. Titanium can be restored only in the central part, where the layer of oxide is relatively thin, but at the edge full recovery does not occur. The situation repeats in the next period of the driving signal. As a result, titanium oxide accumulates mainly at the edge, while the center of the electrode contains less oxide.

3.4 Destruction of the electrodes

The edges of the electrodes tested in the AP regime at f = 50, 100 and 200 kHz have been damaged. The destruction is accompanied by the formation of large particles with a lateral size of several micrometers at the very edge of the electrode and in the close proximity (Fig. 6a-c). These particles have the same chemical composition as the nearby area of the electrode. To all appearance, they are the parts of the electrode that have peeled off from the substrate. Exfoliation can occur under the intrinsic mechanical stress generated in the film during the AP process. The rolled shape of the delaminated edge (Fig. 6b, c) indicates the presence of the stress.

Detachment of thin films from the substrate under the intrinsic stress is a widely known problem in microfabrication [26]. The sources of the stress can be different. It can be induced during the deposition procedure because of crystallographic flaws that are built into the coating [27], or it may develop due to a mismatch of thermal expansion [28]. In our fabrication process Ti demonstrates strong adhesion to the SiO_2 substrate, so the stress generated during the deposition does not lead to exfoliation. Temperature change is also not the case. As shown previously, in the AP electrochemical process the local temperature near the electrodes increases not more than several degrees [9].

The stress has to appear during the growth of the oxide film on the electrode surface. Stress generation during the anodic oxidation of titanium has been described in the literature [29-33]. The stress can have a magnitude as high as several hundred megapascals and cause the breakdown of the film [33]. Several factors responsible for generation of stress are known: the difference in molar volume between TiO_2 and Ti, the different transport numbers of mobile metal and oxygen ions in the film, and the electrostriction effect. The formation of tensile [29] and compressive stress [33] was demonstrated. The stress of both signs is observed in some experiments [30-32], depending on the parameters of electrolysis and the sample preparation method. The rolled shape of the exfoliated edge of the electrode indicates that in our situation the stress is tensile. Hydrogen adsorbed by the titanium oxide film during the cathodic polarization can also significantly affect the internal stress [34].

The chemical composition of the electrodes shown in Fig. 6a-d is presented in Table 2. The data are obtained in zone III near the damaged sites. The highest oxygen content (more than 30 at. %) is observed at the samples tested at f = 50 and 100 kHz. These electrodes demonstrate the strongest destruction. The sample tested at f = 400 kHz has the smallest percentage of O (23 at. %) and is the least damaged. Thus, the higher the oxygen content, the stronger the damage. It is reasonable to assume that the increase in the amount of O means that the oxide layer becomes thicker. Some authors observed an increase of the internal stress with the growth of oxide film [33]. This is probably what happens in our system. The more the electrode is oxidized, the higher stress is developed, and more the electrode suffers. It is worth noting that the anode oxidized in the DC regime does not show any damage. In comparison with the AP process it contains less oxygen (22 at. %, table 1), which is distributed more homogeneously.

Frequency dependence of the oxygen content can also be explained by the misbalance between oxidation and reduction processes. At low frequency the oxidation phase is long, and a thicker layer of titanium oxide builds up on the electrode. The thicker the oxide layer, the harder the reduction process. At higher frequency the oxidation phase is relatively short. A thin oxide layer can be reduced more easily.

Table 2. Chemical composition of the electrodes exposed to the AP electrolysis during T = 60 s. The EDX analysis is performed in zone III, the region of analysis has the size of 3.5×2.5 μm^2. The content of chemical elements is given in atomic percents.

Chemical element	50 kHz	100 kHz	200 kHz	400 kHz
C	5.79	6.1	6.40	5.95
O	34.44	30.2	25.26	22.72
F	7.68	5.0	3.52	2.84
Si	0.85	0.9	1.18	1.80
Ti	50.76	57.4	63.28	66.45

3.5 Current in the electrochemical cell

In the DC process the film of titanium oxide insulates the anode from the electrolyte and the current stops quickly. For the sample shown in Fig. 5, the current has a maximum value of 5 mA at the beginning of the pulse and then it monotonously decreases to zero in about 5 ms. Several visible gas bubbles appear at the cathode. In the AP mode no visible gas is observed at the selected frequencies, while a significant current flows through the electrodes. The waveforms of the current at f = 200 kHz captured at different moments of time are shown in Fig. 9. A sharp peak that occurs in the beginning of the pulse is due to charging-discharging of the double layer on the electrode surface and has no Faraday component responsible for the electrochemical process [20]. The oscillations have a frequency of 10 MHz and are caused by the instability of the amplifier. The plateau of the pulse is due to the Faraday current I_F. However, the pulse changes shape with time. The end of the plateau goes down, forming a characteristic hump (see the waveforms at 25 and 40 s). This hump gradually moves towards the beginning of the pulse. It disappears a minute after the process starts, leaving a low current behind. After this the waveform does not change significantly (see the 80 and 160 s). The current pulse has similar shape at other frequencies.

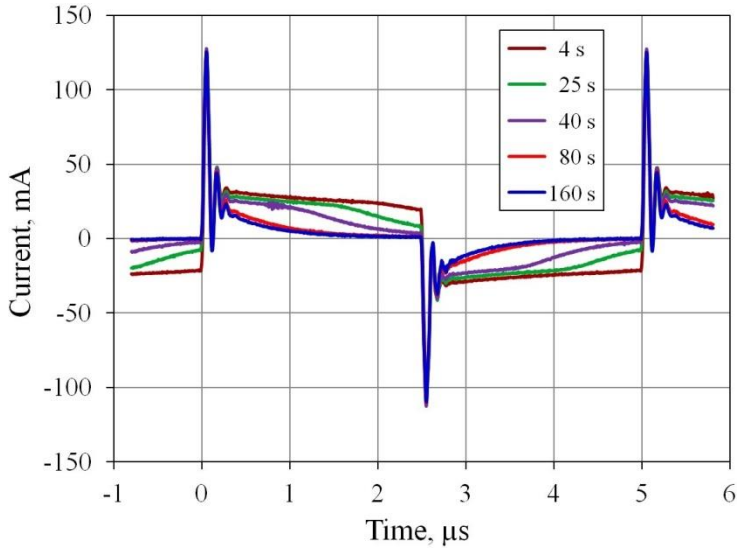

Figure 9. Current flowing through the cell at f = 200 kHz. The waveforms are recorded at 4, 25, 40, 80, and 160 s after the start of the electrochemical process.

If the electrode material is not modified chemically in the electrochemical process, the current flowing through the cell consists of the charging-discharging and Faraday components. It is well fitted by the following time dependence [20]:

$$I(t) = I_F + I_1 e^{-t/\tau_c}, \quad (1)$$

where I_F is the Faraday current, I_1 is a constant and τ_c is the relaxation time related to the capacitance of the double layer. This time dependence works well for the waveforms captured at the beginning and at the end of the AP process, when the plateau does not have the hump. Before fitting, the oscillations are excluded from the signal using a smoothing procedure. For the waveform taken at the fourth

second, we find I_F = 26 mA from the fit. For the waveform taken at 160-th second the approximation gives I_F = 2 mA. One can see that the Faraday current decreases by more than an order of magnitude, but its value is still significant. The 200 μm wide electrode has a surface area of 0.02 mm^2. At I_F = 2 mA the average current density is j_F = 10 A/cm^2, but locally it can be several times higher due to the nonhomogeneous current distribution [20]. This value is much higher than the current density < 0.1 A/cm^2 that is typically used in DC electrochemical actuators [12, 14, 17].

A peculiar shape of the pulse in the intermediate stage of the process (see the waveforms for 25 and 40 s) does not allow extraction of the Faraday current by the method described above. Supposedly, the additional component responsible for the oxidation-reduction process contributes to the current. In order to take this component into account, we use the average current I_{AV} flowing through the electrochemical cell. The waveform is integrated over several periods of the driving signal, and the obtained value is divided by the corresponding time interval. For the negative pulses we take the absolute values of the current. The time dependence of the average current is shown in Fig. 10. The data are plotted for several samples tested at various duration of the process T. In the first seconds of the electrolysis, I_{AV} has the value from 25 to 35 mA. It varies from sample to sample due to slight difference in the thickness of Ti film and pre-treatment of the electrodes. A slight increase of I_{AV} is observed at some samples during the first 15 s of the process, but in most cases it monotonously decreases with time until it reaches the lowest value of 7-13 mA. The current stops changing approximately after 100 s of the process. The average current is always higher than the Faraday current, because it includes all the components. Typically, I_F has the value of 1-2 mA in the steady state.

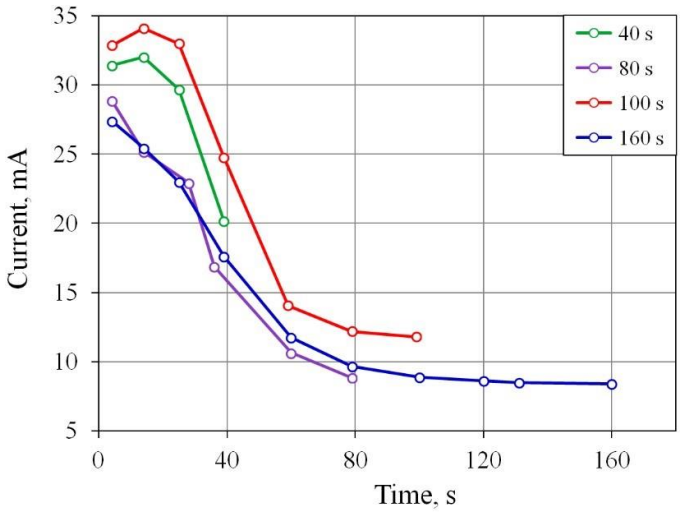

Figure 10. Time dependence of the average current flowing through the electrodes at f = 200 kHz. The data are given for the samples tested at T = 40, 80, 100 and 160 s.

The average current decreases simultaneously with the change of the electrode color. At f = 200 kHz the electrodes darken during the first 40 s of the process (Fig. 4), while the most dramatic

current drop occurs in 60 s (Fig. 10). Formation of titanium oxide on the electrode surface makes the current smaller. As mentioned above, in one half of the period Ti is oxidized, and in the other half it is reduced. The gradual decrease of the current and the darkening of the electrodes indicate that the oxidation process dominates the reduction. However, the current reaches a steady state with time, and the darkening of the electrodes stops. It means that the oxidation and reduction processes compensate each other. The cell maintains this state for hours conducting the Faraday current of the order of 1 mA, while in the DC process the current stops in milliseconds. The ability to conduct the Faraday current in the AP process can be explained by a steady state reached in the oxidation-reduction process. This steady state allows much higher current density than in DC mode, where the reduction process is not involved, and oxide completely blocks the current.

Titanium electrodes exposed to the alternating polarity process differ from those tested in the usual DC regime not only by the spatial distribution, but also by the chemical composition of the material covering the electrodes. As mentioned above, titanium oxide grown in the AP process contains the additives of carbon and fluorine. The sample and the electrolyte contain these elements in residual amounts, but during the electrolysis their local content increases to several percents. C and F can be transferred to the electrodes from the adjacent surfaces and from the electrolyte by convection. Short voltage pulses generate nanobubbles of hydrogen and oxygen over the electrodes. The liquid enriched with these bubbles has a lower mass density than the surrounding electrolyte. It rises up under the buoyancy force, as demonstrated previously [8]. The fluid from the periphery flows into its place. Then it is enriched with nanobubbles, and the situation repeats. Thus, the electrolyte is constantly mixed. In addition, hydrogen and oxygen combined in the same nanobubble disappear in the combustion reaction, releasing a significant energy [20]. This process is absent in the DC electrolysis and also contributes to the convection.

4. CONCLUSIONS

Thin-film titanium electrodes were tested in the electrochemical process performed by microsecond voltage pulses of alternating polarity. The voltage was applied to the working electrode, while the other electrode was grounded. The amplitude of pulses was 9 V, the polarity changed with a frequency between 50 and 400 kHz. Titanium oxide is formed on both electrodes during the process that visually looks like darkening. Unlike normal DC electrolysis, in which the entire surface of the anode is oxidized uniformly, in the AP process the oxide grows at the edges of the electrode more intensively than in the central part. The edge is covered by a continuous oxide layer, while in the middle most of the oxide is collected in separate nanoparticles. The oxidation is accompanied by a gradual decrease of the Faraday current. In the DC process the current drops to zero in milliseconds, while in the AP electrolysis the value of 1-2 mA was kept for hours. The process is interpreted as periodic oxidation and reduction cycles with misbalance in the oxidation part. This explains nonhomogeneous distribution of the oxide over the area of electrode and reduction of the Faraday current with time. Another feature of the AP process was the chemical composition of the titanium oxide. In contrast with the DC electrolysis titanium oxide includes carbon and fluorine additives that

can be connected with active convection during the AP process. The electrodes tested at f = 50 and 100 kHz are damaged during the process, while no damage is observed at f = 400 kHz. The reason for damage that is supported by the EDX analysis is related to tensile stress during the growth of oxide that causes detachment of the edges from the substrate. It is concluded that higher frequency of pulses is preferable to achieve the best durability of titanium electrodes.

ACKNOWLEDGMENTS
This work is supported by the Russian Science Foundation, Grant No. 18-79-10038 and performed using the equipment of Facilities Sharing Centre "Diagnostics of Micro- and Nanostructures".

References

1. S. Trasatti, *J. Electroanal. Chem*., 460 (1999) 1.
2. R. de Levie, *J. Electroanal. Chem*., 476 (1999) 92.
3. K. Zeng and D. Zhang, *Prog. Energy Combust. Sci.*, 36 (2010) 307.
4. M. Wang, Z. Wang, X. Gong and Z. Guo, *Renew. Sust. Energ. Rev*., 29 (2014) 573.
5. T. Kato, M. Kubota, N. Kobayashi and Y. Suzuoki, *Energy*, 30 (2005) 2580.
6. M. Sakurai, T. Terao and Y. Sone, Development of water electrolysis system for oxygen production aimed at energy saving and high safety, 45th International Conference on Environmental Systems, Bellevue, Washington, USA, 2015, 273.
7. V. B. Svetovoy, R. G. P. Sanders, T. S. J. Lammerink and M. C. Elwenspoek, *Phys. Rev.* E, 84 (2011) 035302(R).
8. A. V. Postnikov, I. V. Uvarov, N. V. Penkov and V. B. Svetovoy, *Nanoscale*, 10 (2018) 428.
9. A. V. Postnikov, I. V. Uvarov, M. V. Lokhanin and V. B. Svetovoy, *PLoS ONE*, 12 (2017) e0181727.
10. A. V. Postnikov, I. V. Uvarov, M. V. Lokhanin and V. B. Svetovoy, *Sci. Rep*., 6 (2016) 39381.
11. I. V. Uvarov, M. V. Lokhanin, A. V. Postnikov, A. E. Melenev and V. B. Svetovoy, *Sensor Actuat. B: Chem*., 260 (2018) 12.
12. Y. Yi, U. Buttner and I. G. Foulds, *Lab Chip*, 15 (2015) 3540.
13. R. Sheybani and E. Meng, *Sensor Actuat. B: Chem*., 221 (2015) 914.
14. R. Sheybani, H. Gensler and E. Meng, *Biomed. Microdevices*, 15 (2013) 37.
15. D. E. Lee, S. Soper and W. Wang, *Microsyst. Technol*., 14 (2008) 1751.
16. C. R. Neagu, J. G. E. Gardeniers, M. Elwenspoek and J. J. Kelly, *J. Microelectromech. Syst*., 5 (1996) 2.
17. H. Kim, H. Hwang, S. Baek and D. Kim, *Sensor Actuat. A: Phys*., 277 (2018) 73.
18. C. Lui, S. Stelick, N. Cady and C. Batt, *Lab Chip*, 10 (2010) 74.
19. J. Xie, Y. Miao, J. Shih, Q. He, J. Liu, Y.-C. Tai and T. D. Lee, *Anal. Chem*., 76 (2004) 3756.
20. V. B. Svetovoy, R. G. P. Sanders and M. C. Elwenspoek, *J. Phys.: Condens. Matter*, 25 (2013) 184002.
21. I. V. Uvarov, S. S. Lemekhov, A. E. Melenev and V. B. Svetovoy, *J. Phys.: Conf. Ser*., 757 (2016) 012008.
22. R. Sheybani and E. Meng, *J. Microelectromech. Syst*., 21 (2012) 1197.
23. I. V. Uvarov, S. S. Lemekhov, A. E. Melenev and V. B. Svetovoy, *J. Micromech. Microeng*., 27 (2017) 105009.
24. S. Van Gils, P. Mast, E. Stijns and H. Terryn, *Surf. Coat. Technol.*, 185 (2004) 303.
25. J.-L. Delplancke, M. Degrez, A. Fontana and R. Winand, *Surf. Technol*., 16 (1982) 153.
26. S. D. Senturia, Microsystem design, Springer Science + Business Media, (2001) New York, USA.

27. K. Seshan, Handbook of thin-film deposition processes and techniques, Noyes Publications, (2002) Norwich, USA.
28. F. Dross, J. Robbelein, B. Vandevelde, E. Van Kerschaver, I. Gordon, G. Beaucarne and J. Poortmans, *Appl. Phys. A*, 89 (2007) 149.
29. L. C. Archibald, *Electrochim. Acta*, 22 (1977) 657.
30. S. N. Sahu, J. Scarminio and F. Decker, *J. Electrochem. Soc*., 137 (1990) 1150.
31. J. C. Nelson and R. A. Oriani, *Corros. Sci*., 34 (1993) 307.
32. T. Shibata and Y.-C. Zhu, *Corros. Sci*., 37 (1995) 253.
33. K. Ueno, S.-I. Pyun and M. Seo, *J. Electrochem. Soc.*, 147 (2000) 4519.
34. J.-D. Kim, S.-I. Pyun and M. Seo, *Electrochim. Acta*, 48 (2003) 1123.